Received: 15 July 2020 | Revised: 17 March 2021 | Accepted: 25 March 2021

DOI: 10.1096/fj.202001712RR

RESEARCH ARTICLE

THE FASEB JOURNAL

Perturbation of astroglial Slc38 glutamine transporters by NH_4^+ contributes to neurophysiologic manifestations in acute liver failure

El Hassan Hamdani[1,2] | **Mariusz Popek**[3] | **Małgorzata Frontczak-Baniewicz**[4] | **Tor Paaske Utheim**[5,6] | **Jan Albrecht**[3] | **Magdalena Zielińska**[3] | **Farrukh Abbas Chaudhry**[1,6]

[1]Department of Molecular Medicine, University of Oslo (UiO), Oslo, Norway

[2]Institute of Behavioural Science, Oslo Metropolitan University, Oslo, Norway

[3]Neurotoxicology Department, Mossakowski Medical Research Institute PAS, Warsaw, Poland

[4]Electron Microscopy Platform, Mossakowski Medical Research Institute PAS, Warsaw, Poland

[5]Department of Medical Biochemistry, Oslo University Hospital, Oslo, Norway

[6]Department of Plastic and Reconstructive Surgery, Oslo University Hospital, Oslo, Norway

Correspondence
Magdalena Zielińska, Neurotoxicology Department, Mossakowski Medical Research Centre PAS, Warsaw, Poland.
Email: mzielinska@imdik.pan.pl

Farrukh Abbas Chaudhry, University of Oslo, Department of Molecular Medicine, Institution of Basic Medical Sciences, P.O.Box 1110, 0317 Oslo, Norway.
Email: f.a.chaudhry@medisin.uio.no

Funding information
The National Centre for Research (NCBiR) Polish Norwegian Research Program, Grant/Award Number: Pol-Nor/196190/23/2013; South-Eastern Norway Regional Health Authority, Grant/Award Number: ID 21561/2017052; UiO:Life Science

Abstract

Ammonia is considered the main pathogenic toxin in hepatic encephalopathy (HE). However, the molecular mechanisms involved have been disputed. As altered glutamatergic and GABAergic neurotransmission has been reported in HE, we investigated whether four members of the solute carrier 38 (Slc38) family of amino acid transporters—involved in the replenishment of glutamate and GABA—contribute to ammonia neurotoxicity in HE. We show that ammonium ion exerts multiple actions on the Slc38 transporters: It competes with glutamine for the binding to the system N transporters Slc38a3 and Slc38a5, consequently inhibiting bidirectional astroglial glutamine transport. It also competes with H^+, Na^+, and K^+ for uncoupled permeation through the same transporters, which may perturb astroglial intracellular pH, membrane potential, and K^+-buffering. Knockdown of Slc38a3 in mice results in cerebral cortical edema and disrupted neurotransmitter synthesis mimicking events contributing to HE development. Finally, in a mouse model of acute liver failure (ALF), we demonstrate the downregulation of Slc38a3 protein, impeded astroglial

Abbreviations: ADC, apparent diffusion coefficient; ALF, acute liver failure; AOM, azoxymethane; BBB, blood–brain barrier; C, control; CNS, central nervous system; CLF, chronic liver failure; DARTS, the Drug Affinity Responsive Target Stability; EM, electron microscopy; GAH, L-glutamic acid γ-monohydroxamate; GS, glutamine synthetase; HE, hepatic encephalopathy; HEK, human embryonic kidney cells; MRS, magnetic resonance spectroscopy; NH4+, ammonium ions; NKCC1, Na^+-K^+-$2Cl^-$ co-transporter isoform 1; SA1-2, System A transporter 1-2; SAT1-2, System A transporter 1-2; Slc, solute carrier family; Slc38a1-a5, solute carrier family member 1-5; SN1-2, system N transporter 1-2; SNAT1-5, sodium-coupled amino acid transporter 1-5; TEVC, two-electrode voltage-clamp; VM, vivo-morpholino oligonucleotides; X., Xenopus.

El Hassan Hamdani and Mariusz Popek contributed equally to this work.

glutamine release, and cytotoxic edema. Altogether, we demonstrate contribution of Slc38 transporters to the ammonia-induced impairment of glutamine recycling between astrocytes and neurons, a phenomenon underlying acute ammonia neurotoxicity in the setting of ALF.

KEYWORDS

hepatic encephalopathy, NH_4^+, Slc38, Slc38a3, SNAT3

1 | INTRODUCTION

Hepatic encephalopathy is a spectrum of metabolic encephalopathies due to acute liver failure (ALF) or chronic liver failure (CLF).[1] Whereas CLF develops over time due to damage of liver tissue, eventually leading to liver cirrhosis, ALF is usually induced by hepatotoxins in patients with no prior liver disease and develops quickly into increased intracranial pressure and life-threatening cerebral edema.[1,2] In ALF, although there is support for many causes and targets, toxic level of ammonium ions (NH_4^+) in equilibrium with ammonia—further referred to as ammonia—is considered the main pathogenic factor[3,4] and correlates well with the clinical phenotype.[5,6]

Ammonia—generated as a by-product of protein catabolism primarily in the enterocytes and gut microbiota—is detoxified under normal physiological conditions in the liver.[7] In liver dysfunction, ammonia is no longer detoxified in the liver but builds up in the blood and accumulates in the central nervous system (CNS).[8] In the brain, glutamine synthetase (GS), an enzyme catalyzing fusion of ammonia with glutamate to form glutamine is mainly located in astrocytes[9], rendering astroglia a main detoxification site for ammonia.[10] However, the resulting high concentration of glutamine is also considered to critically contribute to the development of brain edema in HE: glutamine inflicts osmotic stress on astroglial cells (the osmotic gliopathy theory)[11] or it may be transported into the mitochondria where ammonia may be regenerated and have detrimental effects on mitochondrial functions (The Trojan horse hypothesis).[12] It has also been reported that ammonia neurotoxicity impairs astrocytic potassium buffering and that the increased extracellular K^+ then over-activates neuronal Na^+-K^+-$2Cl^-$ co-transporter.[13] As a result, GABA reversal potential is depolarized, which impairs cortical inhibitory networks and results in HE.[13] However, current hypotheses only explain HE partially.

We have characterized several members of the Slc38 family and have shown that the system N transporters Slc38a3 (also known as (aka) SN1 or SNAT3) and Slc38a5 (aka SN2 or SNAT5) reside on membranes of astroglia and Müller glia cells and mediate bidirectional electroneutral glutamine transport to furnish neurons with glutamine.[14-16] The homologous system A transporters are enriched on neurons and accumulate glutamine: Slc38a1 (aka SAT1 or SA2 or SNAT1) sustains GABA synthesis in GABAergic neurons and contributes to presynaptic plasticity,[17,18] while Slc38a2 (aka SAT2 or SA1 or SNAT2)—enriched on dendrites of glutamatergic neurons—transports glutamine to form glutamate for retrograde signaling.[19-21] As altered GABAergic and glutamatergic neurotransmission has been demonstrated in HE,[22,23] we hypothesized that NH_4^+ may target the Slc38 transporters, thereby impairing astroglial-to-neuronal shuttling of glutamine that, in turn, leads to glutamine toxicity in astroglia and disabled neurotransmitter synthesis in neurons. The consequently perturbed neurotransmission could be consistent with the biphasic nature of HE, where initial overexcitation reflecting increased glutamatergic tone that evolves to neural inhibition associated with more active GABAergic transmission.[4] We have therefore investigated the impact of NH_4^+ on the function and expression of four synapse-associated Slc38 transporters and characterized the phenotype of mice with local depletion of Slc38a3 and a mouse model for ALF. Collectively, our data suggest the involvement of isoform-specific regulation of Slc38 transporters in response to excess ammonia accumulation in the brain associated with ALF.

2 | MATERIALS AND METHODS

2.1 | Preparation of *Xenopus* (*X.*) oocytes and electrophysiological recordings

Female *X. laevis* were purchased from Xenopus 1, Dexter, MI, USA and kept at the Institute of Basic Medical Sciences, University of Oslo, in accordance with national legislation and institutional guidelines at the University of Oslo. Dissection, treatment, and recordings from oocytes were done as previously described.[16] Briefly, the ovarian tissue was removed under anesthesia by immersion of the frog in 1% MS-222 (Sigma–Aldrich, St. Louis, MO, USA), and Stage V and VI oocytes were isolated by collagenase. cDNA encoding Slc38a1-3 and Slc38a5 was subcloned into either the modified pGEM-3ZHE or pGEM-4Z vectors[24,25] (Promega, Madison, WI, USA), and cRNA was synthesized in vitro using the T7 mMessage mMachine kit (Ambion, Austin, TX,

USA). Oocytes were injected with 5-15 ng cRNA using the microinjector FemtoJet (Eppendorf, NY, USA) and incubated at 16°C for 5 to 10 days in modified Barth's medium (90 mM NaCl, 1 mM KCl, 0.82 mM $MgCl_2$, 0.74 mM $CaCl_2$, 0.66 $NaNO_3$, 2.4 mM $NaHCO_3$, 10 mM HEPES, 2.5 mM pyruvate, 5 mL Penicillin–Streptomycin solution, pH 7.5). Control oocytes were injected with equivalent amounts of water or were non-injected.

2.2 | Electrophysiological recordings

Whole cell two-electrode voltage clamp recordings were performed at room temperature using the oocyte clamp amplifier OC-725C (Warner Instruments, Hamden, USA). Signals were digitized using the Digidata 1322A A/D converter (Axon Instruments, Union City, CA) and acquired using the pCLAMP 10 software (Axon Instruments, Union City, CA). Current and voltage pipettes made from borosilicate glass capillary (O.D. 1.5 mm, I.D. 1.1 mm) were backfilled with 3M KCl and had a resistance between 1 and 2 MΩ. In these experiments, ND96 (96 mM NaCl, 2 mM KCl, 1.8 mM $CaCl_2$, 1 mM $MgCl_2$, and 5 mM HEPES pH 7.5) was used as perfusate except when modified by NH_4Cl as mentioned elsewhere in the text. Voltage jumps were applied from a holding potential of −40 mV in increments of 20 mV ranging from −140 to +40 mV. The presented currents were determined by subtraction of steady-state current measurements in the absence of substrates from those in the presence of substrates. The results presented in the figures are each representative of at least three independent experiments.

2.3 | Primary cultures of Müller cells

Rat eyes were collected and connective tissue was removed. Eyes were then immersed in ice-cold serum-free DMEM. Subsequently, anterior segment and vitreous were removed under the dissecting microscope. The retina was dissected out and rinsed with ice-cold serum-free DMEM and collected by centrifuging at 1000 rpm for 5 minutes. Müller glia cells were then isolated by trypsin dissociation at 37°C for 20 minutes with occasional trituration. Cells were then washed 2 times and plated on poly-D lysin coated T75 cm^2 flasks and incubated at 37°C with 5% CO_2. Culture media were replaced every 2-3 day, and microglial cells were removed from the culture after a week. Purified Müller glia cells were then used for the experiment.

2.4 | pHi fluorescence microscopy

Müller glia cells and stably transfected PS120 cells expressing Slc38a3 or Slc38a5 were imaged as previously described.[14] The cells were loaded for 15 minutes with 5 μM BCECF-AM (Invitrogen, Paisley, UK) in Krebs-Ringer (120 NaCl, 4.7 KCl, 2.2 $CaCl_2$, 1.2 $MgSO_4$, 1.2 KH_2PO_4, 10 HEPES, 0.18% glucose pH 8.0), washed for 10 minutes, and monitored by ratiometric imaging at 440 nm and 490 nm excitation and emission at 530 nm using $Cell^R$ system connected to an IX81 motorized inverted microscope (Olympus, Japan).

2.5 | Cell cultures and transfection

PS120-cells derived from hamster lung fibroblast line CCL-39 26 were stably transfected with Slc38a1-a3 or Slc38a5 using lipofectamine 2000-CD (Invitrogen) and were grown in Dulbecco's modified Eagles medium (DMEM) containing 5% fetal bovine serum and 1% penicillin–streptomycin.[16,26] Human embryonic kidney (HEK) cells were grown in DMEM (high glucose with UltraGlutamine, Lonza) supplied with 10% FBS and penicillin–streptomycine (ThermoFisher Scientific) at 37°C and 5% CO_2). HEK293T cells were seeded at a density of 0.5×10^3 cells mm^{-2} on poly-D-lysine-coated plates 24 hours prior to transfection. The cells were transfected with 0.25 μg plasmid DNA per well (for 24-well plates, or scaled accordingly) using Lipofectamine LTX with PLUS-reagent (Life Technologies) following the manufacturer's instructions and incubated for 20-48 hours. Cells were transfected with N-terminally Flag-tagged Slc38a1 (pCMV-Tag1), Slc38a2 (pFLAG-CMV2), and Slc38a3 (pCMV-Tag1), and C-terminally Myc-tagged SN2 (pCMV-tag5a). PS120 cells stably transfected with Slc38a3 and Slc38a5[16,26] were cultured with additional supply of 400 μg mL^{-1} G418/Geneticin (ThermoFisher Scientific).

2.6 | Amino acid uptake and efflux experiments

Slc38a1, Slc38a2, or mock transfected HEK293T cells were washed three times in Krebs-Ringer solution (140 mM NaCl, 4 mM KCl, 2.2 mM $CaCl_2$, 1.2 mM $MgSO_4$, 1.2 mM, KH_2PO_4, 10 mM HEPES, 5.55 mM glucose pH 7.4) and incubated in various concentrations of NH_4Cl for 2 minutes, before adding 2 mM MeAiB (containing 2 μM ^{14}C-labeled MeAiB) for 10 minutes. Slc38a3, Slc38a5, or mock transfected HEK293T cells, wild-type or stably transfected PS120 cells were washed three times in Krebs-Ringer solution with sodium replaced with lithium (140 mM LiCl, 4 mM KCl, 2.2 mM $CaCl_2$, 1.2 mM $MgSO_4$, 1.2 mM KH_2PO_4, 10 mM HEPES, 5.55 mM glucose pH 7.4 or 8) and incubated in various concentrations of NH_4Cl for 2 minutes, before adding 2 mM Gln (containing 0.04 μM ^3H-labeled Gln) for 10 minutes. The reactions were terminated by three ice-cold washes in the same buffer, and the

cells were lysed in 200 μL HEPES buffer pH 8 with 1% Triton X-100 and 0.1% SDS. Protein concentrations were measured with DC protein assay (Bio-Rad), and the radioactivity was measured by scintillation counting in 2.5 mL Optifluor (Perkin–Elmer). To measure glutamine efflux, wild-type or stably-transfected cells were incubated in full growth medium supplied with 2 mM Gln (containing 0.04 μM ^{3}H-labeled Gln) for 90 minutes, washed three times in ice cold Krebs-Ringer solution with lithium (pH 8), and incubated various time points with or without 5 mM NH_4Cl. The reaction was stopped by harvesting the supernatant, washing the cells, and lysing them as described above. Net efflux was assessed in terms of the relative difference of supernatant glutamine-concentrations from cells incubated for no minutes and 30 minutes. The same experiment was performed with MeAiB loaded cells as a control.

2.7 | Drug affinity responsive target stability (DARTS)

Intact cells were washed incubated with 0.5-10 mM NH_4Cl and/or 5 mM glutamine in EBSS buffer (Thermo Fisher Scientific) for 2-5 minutes on ice. To avoid denaturation of the membrane proteins, the transporters were isolated in a mild lysing buffer containing 2.5 mM $CaCl_2$, 100 mM NaCl, 1% Triton-X100, 1×EDTA-free phosphatase inhibitors (Roche), and 10 mM HEPES (pH 7.4), supplied with the same concentrations of NH_4Cl and glutamine, for 1 hour. The lysates were prepared by centrifugation and the DARTS protocol was followed as previously reported.[27] The protein lysates were digested with 0.5, 2.5, or 10 μg mL^{-1} Thermolysine (Sigma) at ice or RT for various time points. One time sample buffer supplied with EDTA and DTT was added to stop the reaction, and was followed by western blotting.

2.8 | Western blot

Cells expressing Slc38a3 were washed three times with phosphate buffered saline (PBS), harvested, and homogenized with BugBuster buffer (Novagen) supplemented with cOmplete ULTRA Tablet, Mini, *EASYpack* Protease Inhibitor Cocktail (Roche, cat. no. 05892970001) and PhosSTOP tablet (Roche, cat. No 04906845001). Proteins were separated in 10% Criterion TGX Precast Midi Protein Gel gels (Biorad, cat. no. 5671034), and gels were run at 220V for 35 minutes. Proteins were transferred to nitrocellulose membranes (Biorad, cat.no. 1620112) and blocked with 5% non-fat dry milk in Tris-buffer saline (TBS) for 1 hours at room temperature. Membranes were probed with home-made purified antibodies [rat anti-Slc38a3 (final concentration: 1μg/mL)].[40] Blots were incubated overnight at 4°C before incubation with a secondary anti-rabbit IgG (dilution 1:40 000; Thermo Fischer Scientific; cat. no. 31460) conjugated with horseradish peroxidase (HRP) for 2 hours at room temperature. Blots were washed 3× with TBS-0,5% Tween after the primary and secondary antibodies. Signals were detected with the SuperSignal West Femto Chemiluminiscent substrate (Thermo Fischer Scientific, cat. no. 34087) and developed at Biorad ChemiDoc imager.

2.9 | Immunofluorescence staining

Treated cells were fixated with 4% paraformaldehyde at room temperature for 30 minutes, washed three times with phosphate buffered saline (PBS), and stained with home-made and purified primary antibodies raised against rat Slc38a3 (final concentration: 2 μg/mL).[40] After the primary antibody incubation, cells were incubated with Alexa Fluor 488 goat anti-rabbit IgG (Thermo Fischer Scientific, cat. no. 702323) before visualization of the fluorescence signal by confocal microscopy (Zeiss LSM 510 META; Carl Zeiss AS). Nuclei were counterstained with DAPI and cells were mounted with Prolong gold (ThermoFischer Scientific, cat. no.) onto microscope slides.

2.10 | Study design and animal groups

Animals were randomly divided into four experimental groups: control to AOM mice (27), AOM mice (27), VM control (18), and Slc38a3-VM (18). Isolated cortex studies were conducted on eight control and eight AOM mice or three C-VM and three Slc38a3-VM mice; ultrastructural analysis was carried out on four control, four AOM, three C-VM, and three Slc38a3-VM mice; MRI studies were done on nine control, nine AOM, seven C-VM, and seven Slc38a3-VM mice; microdialysis study was carried out on 5 C-VM and 5 Slc38a3-VM mice; glutamine transport analysis were studied on six control and six AOM mice, respectively. Number of animals was determined based on pilot studies which provided statistically significant differences between test and control. For transmission electron microscopy experiments, MRI analysis, and HPLC studies, the researchers analyzing samples were entirely blinded to the experimental groups.

2.11 | Experimental mouse models

All experiments were performed with agreement of local animal ethical committee in Warsaw in accordance with EC Directive 86/609/EEC. Male C57Bl6 mice (animal colony of the Mossakowski Medical Research Centre, Polish Academy of Sciences in Warsaw), body weight 30.0 ± 5.1 g, were kept 3-4 under standard laboratory conditions in cages model 1291H Eurostandard Type III H at room temperature (22°C).

1. AOM model of acute liver failure in mice

ALF was induced via a single intraperitoneal injection of 100 mg/kg of azoxymethane (AOM) into 27 mice exactly as described previously.[28] Experiments were performed at the pre-comatose stage of HE (grade IV ALF; 20-22 hours after AOM injection), a time point selected based on the neurological assessment of mice. The reflexes: startle, righting, postural, corneal, pinna and vibrissae, were analyzed exactly as described earlier.[28]

2. *vivo-morpholinos* (VM) model of local Slc38a3 protein silencing in frontal cortex of mice

For VM models of local Slc38a3 protein silencing in frontal cortex *of mice*: 36 C57Bl6 mice were anesthetized (2% isoflurane) and subjected to subcutaneous implantation (coordinates: AP +2.0, ML −0.8, DV −1.5) of osmotic pumps (no. 1002; Alzet, Cupertino, CA) that continuously infused 100 µL anti-Slc38a3 vivo-morpholino oligonucleotides (Slc38a3-VM) (sequence: 5′ ATGGCTCAGAGACCACCCCAGAACA 3′ and 5′ CTGCTCTCACACTGACAGTCAGGTA 3′; Gene-Tools LLC Summerton Way Philomath, OR, USA; 1.2 mg/kg/day for 4 days) or mismatched-VM. For VM experiments the endpoint was after 96 hours, mice were euthanized, and tissue was collected.

2.12 | Ammonia level determination

Control and AOM mice were anesthetized, and 1 cm incision was made on the neck. After immobilization of animal's head, cerebral spinal fluid (CSF) (5-10 µL) was collected by Pasteur pipette from the cisterna magna area. Subsequently blood was assembled and set aside to form a clot, followed by centrifugation for 10 minutes in 3000 ×*g*. Then ammonia was immediately measured spectrophotometrically in CSF and serum samples using Ammonia Assay Kit (Sigma Aldrich, Poznań, Poland) at the 340 nm wavelength.

2.13 | Immunoblotting analyses

After decapitation, immediately removed mice brain cortex was isolated on ice. An area of interest: a fragment surrounding the probe outlet 2 mm/2 mm and ~5 mg of weight was dissected from Slc38a3-VM, control, and AOM mice (ipsilateral cerebral hemisphere were also dissected for comparison). Tissue samples were homogenized in buffer (20 mM Tris–HCl pH 6.8; 137 mM NaCl; 2 mM EDTA; 1% Triton X-100; 0.5 mM DTT; 0.5 mM PMSF; Phosphatase Inhibitor cocktail 2 (1:100, P5726, Sigma–Aldrich, Poznań, Poland), Protease Inhibitor Cocktail (1:200, P8340, Sigma– Aldrich, Poznań, Poland)) and centrifuged at 12000 ×*g* for 10 minutes. Protein concentrations were performed using a BCA Protein Assay (Thermo Fisher Scientific; Warsaw, Poland). Proteins content was assessed by immunoblotting as previously described.[29] Membranes were blocked in 5% milk and incubated overnight at 4°C with antibodies for Slc38a3 (1:1000, 14315-1-AP, ProteinTech, Manchester, UK), Slc38a2 (1:200, sc-166366, Santa Cruz Biotechnologies, Dallas, TX, USA) in dilution in 1% milk and then for 1 h in 1% milk with HRP-conjugated-anti-goat IgG (1: 2500, sc-2020, Sigma-Aldrich, Poznań, Poland) and HRP-conjugated goat anti mouse, A28177 (1: 5000; Thermo Fisher Scientific), respectively. Data were expressed as fold change in fluorescent band intensity of target antibody divided by GAPDH (1:7500, HRP-60004, ProteinTech, Manchester, UK) used as a loading control. Band intensity quantifications were analyzed using GeneTools software (SynGene).

2.14 | Real-time PCR analysis

RNA was extracted from dissected tissue using TRI reagent (Sigma–Aldrich, Poznań, Poland) and reverse-transcribed using a High Capacity cDNA Reverse Transcription Kit (Applied Biosystems, Waltham, MA, USA). Real-time PCR was performed as previously described[28,29] using commercially available primers designed against mouse Slc38a3 and β-actin (Applied Biosystems). A ΔΔCT analysis was performed using vehicle-treated tissue as controls experiments.[30]

2.15 | Transmission electron microscopy

The animals were anaesthetized and perfused through the ascending aorta with 2% paraformaldehyde and 2.5 % glutaraldehyde in 0.1 M cacodylate buffer, pH 7.4. Perfused mice brains were sliced, fixed, and placed in a mixture of 1% OsO_4 and 0.8% $K_4[Fe(CN)_6]$ as previously described.[28] Sections (blood vessels and astrocytes) were morphologically analyzed in specimens from control, AOM, C-VM, and Slc38a3-VM mice. The percentage of blood vessel profiles (n = 50 for each group) and astroglial cell profiles that were morphologically changed was calculated for each group.

2.16 | Metabolite analysis by ^{1}H magnetic resonance spectroscopy

To obtain the spectra of brain metabolites, localized proton spectroscopy (Biospec 70/30USR) at short echo was performed using PRESS sequence (TR/TE = 2000/20 ms, 512 averages, 2048 points, scan time = 17 min) with VAPOR water suppression, the outer volume suppression, and

frequency drift correction (flip angle 5°). Measurements were carried out in two separated volumes of interest (VOI; $2 \times 2 \times 1.5$ mm^3) encompassing the pertinent, silenced regions of frontal cortex. Linear and second-order global shims were adjusted with ADJ_1st_2nd_order protocol. Afterwards, linear and second-order local shims were automatically adjusted with FASTMAP in a cubic volume that contained the volume of interest region ($2 \times 2 \times 2$ mm^3 for the frontal cortex). Metabolite concentrations were determined using a linear combination analysis method LCModel[31] (http://www.s-provencher.com/pages/lcmodel.shtml). Unsuppressed water signal measured from the same volume of interest was used as an internal reference for absolute metabolite quantification. Metabolite concentrations are reported in institutional units (i.u.). The spectra signal-to-noise ratio was typically at around 12-25.

2.17 | Determination of apparent diffusion coefficient (ADC)

Brains were scanned with Bruker BioSpec 70/30 Avance III system working at 7T with a transmit cylindrical radiofrequency coil (8.6 cm inner diameter) and a mouse brain dedicated receive-only array coil (2×2 elements) placed over the animal's head. The animals were positioned prone with the head placed in the stereotactic apparatus and were anesthetized (1.5-2% isoflurane in air). Structural transverse MR images covering the whole brain were acquired with T2-weighted TurboRARE (TR/TE = 6000/30 ms, RARE factor = 4, spatial resolution = $78 \times 78 \times 500$ µm, 35 slices, no gaps, number of averages (NA) = 4, scan time = 25 minutes). Spin echo diffusion-weighted images covering the whole brain were acquired (TR/TE = 7000/27 ms, *b*-values = 0, 600, 1110 s/mm^2, number of directions = 1, spatial resolution = $156 \times 156 \times 700$ µm, 25 slices, no gaps, scan time = 33 minutes). ADC maps were calculated by mono-exponential fitting of the three experimental points using Bruker ParaVision 5.1 software. The data were processed using SPM software (www.fil.ion.ucl.ac.uk/spm/). ADC maps were registered (rigid transformation) to the structural T2-weigthed images and normalized (affine transformation) to the 3D in vivo mouse brain template space (MRM NeAt database). Each individual brain structures atlas was obtained by automatic labeling whole brain using MRM NeAt atlas and transformation matrix (obtained in the normalization step). That automatic labeling algorithm was implemented as custom-made MATLAB script (http://www.mathworks.com/products/matlab/) exploiting modified functions provided by IBASPM software (http://www.thomaskoenig.ch/Lester/ibaspm.htm). ADC maps were overlaid with the corresponding atlas, and mean ADC values from each structure voxels were calculated using custom-made MATLAB scripts as previously described.[32] For control and AOM mice, we analysed whole cortex region, and for C-VM and Slc38a3-VM we choose pertinent region of an appropriate, selected region of the brain around the probe outlet with a field of approximately $2 \times 2 \times 2$, excluding the hole remaining after the cannula, and the corresponding place in the other cerebral hemisphere, comparably.

2.18 | Microdialysis on freely moving mice

After osmotic pump implantation at coordinates AP +2.1, ML −0.8, in a close proximity to probe inlet, a guide cannula to microdialysis was implanted at a depth of 0.5 mm. Before arousals, antibiotic (Baytril, 2.5%; 0.2 mL/kg of body weight) and a painkiller (Ketoprofen 5 mg/kg of body weight) were subcutaneously administered. 96 hours after surgery, mice were anesthetized with isoflurane (3.5% in air) and probe was implanted. ACSF of the following composition (in mM): NaCl (130), KCl (5), $CaCl_2$ (2.5), $MgSO_4$ (1.3), KH_2PO_4 (1.25), $NaHCO_3$ (26), and D-glucose (10), aerated with mixture of 95% O_2 and 5% CO_2 was passed through the probe. Microdialysates were collected every 40 minutes (100 µL) for 4 hours (6 fractions) and immediately frozen at −80°C.

2.19 | High-performance liquid chromatography determination of amino acids

Amino acid concentration in microdialysates was measured using HPLC with fluorescence detection after derivatization in a timed reaction with *o*-phthalaldehyde with mercaptoethanol, exactly as described earlier.[32] Samples (50 µL) were then injected on to a 5 µm Bio-Sil C18 Hl column (250 × 4.6 mm, BIO-RAD), with a mobile phase of 0.075 M KH_2PO_4 solution containing 10% v/v methanol, pH 6.2 (solvent A), and methanol (solvent B).

2.20 | Glutamine transport analysis

The brains from AOM and control mice were isolated (as described in Immunoblotting analyses section) and immediately immersed in Krebs buffer of the following composition (in mM): NaCl (150); KCl (3); $CaCl_2$ (2); $MgCl_2$ (0.8); glucose (5); Hepes (10) aerated with 95% O_2 and 5% CO_2 at pH 7.4, temp. 37 ± 0.5°C. Dissected prefrontal cortex was then cut into sections, 350 µm thick. Cortical micro-slices were pre-incubated in a Krebs buffer for 30 minutes. L-[^{3}H] glutamine efflux was measured after 30 minutes incubation in Krebs buffer containing 0.5 µCi/mL L-[3,4-^{3}H(N)-] glutamine (PerkinElmer, Waltham, MA, USA; specific radioactivity 37 MBq/mL), unlabeled Gln (100 µmol/L), and

in the presence/absence of alanine, leucine or L-glutamic acid γ-monohydroxamate (GAH, Sigma Aldrich) at 5 mM concentration. Slices were then transferred to a chamber perfusion system (Brandel, USA) and superfused with Krebs buffer at 0.5 mL/min rate. After draining 10 minutes. of the initial fraction, 1-min perfusate samples were collected for 10 minutes at a rate of 0.5 mL/min. In some variant, from four fractions the Krebs buffer contained 5 mM L-alanine and 5mM L-leucine or 5mM GAH. Radioactivity released from the preparations and brain sections were measured by a Wallac 1409 (Perkin–Elmer, Turku, Finland) liquid scintillation counter.

2.21 | Statistical analysis

All experiments were carried out with replicates depending on the experiment type. No test for outliers was conducted on the data obtained in the study. Normal distribution was checked in each group using the Shapiro–Wilk test. When two populations groups of responses were examined, depending on the results obtained, Student's *t* test or the Mann-Whitney *U* test was applied (see legends to figures). Error bars represent the SEM, which is specifically indicated, $*P < .05$, $**P < .01$, and $***P < .001$. All statistical analyses were performed using Statistica software package (Statsoft Inc., USA) and GraphPad Prism 7 (GraphPad Software, Inc., USA).

3 | RESULTS

3.1 | NH_4^+ inhibits bidirectional glutamine transport by two astroglial system N transporters

A perturbation of astroglia-to-neuron shuttling of glutamine would lead to dysfunctional glutamatergic and/or GABAergic neurotransmission—a hallmark of HE. Four Slc38 transporters associated with fast synaptic neurotransmission have been characterized by two-electrode voltage-clamp electrophysiology (TEVC) upon heterologous expression in *X. laevis* oocytes.[15,16,25,33] We therefore applied TEVC to investigate whether NH_4^+ affects the function of these four transporters, which could perturb fast neurotransmission. Ammonium ion concentrations up to 8 mM have barely any impact on the glutamine-induced currents in oocytes expressing the system A transporters Slc38a1 or Slc38a2 (Figure 1A,B). In contrast to this, NH_4^+ dramatically affects the activity of the system N transporters: Incubation with 4 mM NH_4^+ reduces the glutamine-induced currents in Slc38a3 and Slc38a5 expressing oocytes significantly, while 8 mM NH_4^+ abolishes them (Figure 1C,D). We also tested whether the inhibition of Slc38a3 function is due to a distinct NH_4^+ effect on Slc38a3 or it is a secondary consequence of a change in intracellular pH (pH_i) reducing the driving force of Slc38a3 transport. Ammonia and trimethylamine (TMA) are both weak bases and increase pH_i to similar extent.[34] In contrast to ammonia, TMA has no effect on Slc38a3 activity (Figure 1E), implicating that ammonia act on Slc38a3 and does not work indirectly through change in pH_i.

Slc38a3 and Slc38a5 mediate electroneutral and bidirectional amino acid transport. However, the glutamine-induced currents seen in *X. laevis* oocytes are due to uncoupled ion fluxes permeating through the same transporters gated by the amino acid substrates.[14,15,16,35] To pinpoint whether NH_4^+ targets the transport activity, the channel activity or both, we scrutinized transport of radiolabeled substrates in mammalian cells expressing Slc38 transporters. HEK cells transiently transfected for Slc38a1 or Slc38a2 display a significantly higher uptake of MeAIB—a prototypic System A substrate—than mock transfected cells (Figure 2A). Such transport persists even upon co-incubation with NH_4^+. This is consistent with data obtained by TEVC electrophysiology showing lack of inhibition of the system A transporters by NH_4^+ (Figure 1A,B).

PS120 cells stably transfected for Slc38a3 and Slc38a5 transport significantly more glutamine compared with mock transfected cells (Figure 2B).[14,16] Co-incubation with ammonium ions reduces the Slc38a3- and Slc38a5-mediated glutamine transport significantly (Figure 2B). We also investigated glutamine efflux by the system N transporters: Cells expressing Slc38a3 or Slc38a5 are capable of significant glutamine release (Figure 2C), which is in harmony with earlier reports.[14,16,29] Interestingly, ammonium ions impairs the release mode of the two system N transporters as well (Figure 2C). Altogether, our data demonstrate that ammonium ions abolishes selectively Slc38a3- and Slc38a5-mediated bidirectional substrate transport and associated uncoupled currents while it has no impact on Slc38a1 or Slc38a2 transport activity.

3.2 | NH_4^+ competes with other cations for uncoupled fluxes through the system N transporters

Uncoupled transporter-associated cation-fluxes are a hallmark of Slc38a3 and Slc38a5 transporters.[15,16,33] We therefore hypothesized that NH_4^+ also permeates through Slc38a3 and Slc38a5. In the presence of Na^+ but without glutamine in the incubation buffer, addition of NH_4^+ did not change the reversal potential (data not shown). However, as Na^+ itself permeates through Slc38a3,[15,33] and may compete with NH_4^+ fluxes; we re-tested NH_4^+ fluxes through Slc38a3 in the absence of Na^+ and amino acid substrates in the incubation buffer. Now, increasing the concentrations of NH_4^+ shifts the reversal potential stepwise toward depolarized potentials

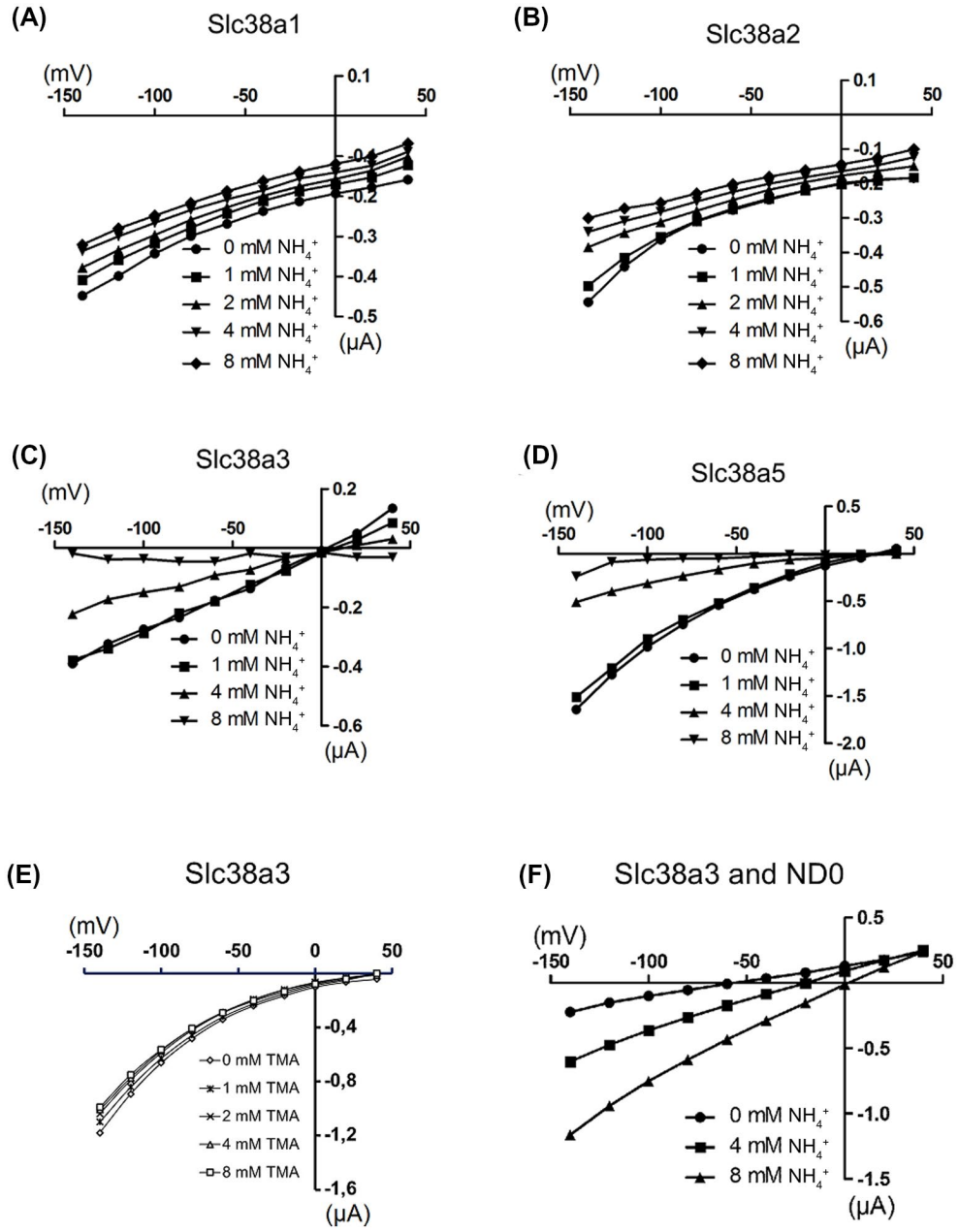

FIGURE 1 NH_4^+ inhibits selectively the substrate-induced currents associated with the system N transporters Slc38a3 and Slc38a5 and it penetrates through them uncoupled to transport. *Xenopus (X.) laevis* oocytes injected with in vitro transcribed mRNA for one of four Slc38 transporters were incubated with glutamine (5 mM) and subjected to two-electrode voltage-clamp electrophysiology. Voltage jumps were generated from a holding potential of −40 mV in increments of 20 mV ranging from −140 mV to +40 mV and voltage-current relationships were measured. A-D,Glutamine generates currents in oocytes expressing either of Slc38a1, Slc38a2, Slc38a3, or Slc38a5 transporters. Co-incubation with ammonium (1, 2, 4, or 8 mM) has only minor effects on the currents associated with Slc38a1 or Slc38a2 transporters. By contrast, ammonium abolishes glutamine-induced currents in oocytes expressing Slc38a3 or Slc38a5 transporters in a concentration-dependent manner. E, *X. leavis* oocytes injected for Slc38a3 and stimulated with glutamine show large inward currents at negative membrane potentials. Co-incubation with trimethylamine (TMA) has no impact on the glutamine-induced currents. F, Voltage-current measurements in *X. leavis* oocytes expressing Slc38a3 were performed in the absence of Na^+ and glutamine. Rising ammonium concentrations increases the current magnitude and shifts the reversal potential toward positive values

(Figure 1F) and the reversal potential for NH_4^+,[36] confirming channeling of NH_4^+ through Slc38a3.

High levels of ammonia were required to show effect on the two system N transporters when they were expressed in *X. laevis* oocytes (Figure 1). We therefore turned to test effect of clinically relevant ammonia levels in glial-like cells with endogenous system N activity. Müller glia cells are astroglia-like cells of the retina and a part of the central nervous system: They

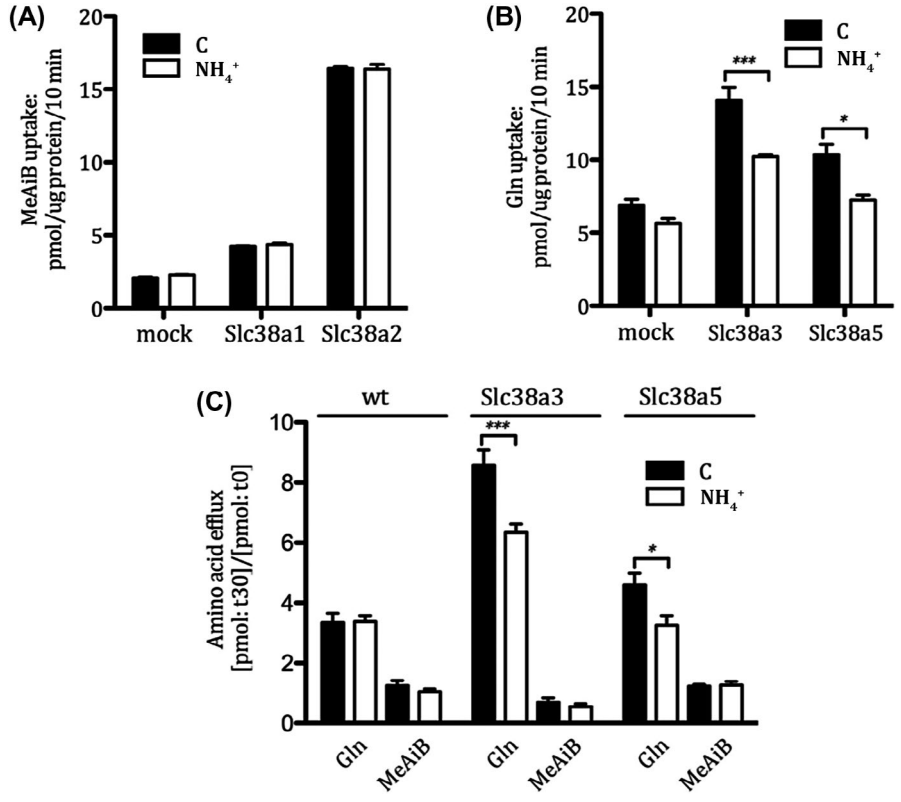

FIGURE 2 Isoform-specific impact of ammonium on Slc38 transporter activity. A-B, Mammalian cells mock transfected or transfected for one of the Slc38 transporters were treated with or without ammonium and incubated with a radiolabeled substrate (2 mM MeAIB or 2 mM glutamine) followed by cell lysis in SDS and measurement of the accumulated substrate in a scintillation counter. A, MeAIB is accumulated to a significantly higher degree in Slc38a1 or Slc38a2 transfected cells compared with mock-transfected cells. Co-incubation with ammonium has no impact on transport activity. B, PS120 cells stably transfected for Slc38a3 or Slc38a5 accumulate significantly more glutamine than the mock-transfected control cells. Co-incubation with ammonium significantly reduces glutamine uptake in cells expressing Slc38a3 or Slc38a5. C, Slc38a3, Slc38a5, or mock transfected PS120 cells were loaded with radiolabeled glutamine or MeAIB for 1.5 hours followed by incubation in amino acid-free buffer with or without 5 mM NH_4Cl. Net efflux was calculated as the concentration in the supernatant after 30 minutes over 0 minutes. MeAIB was used as a non-system N substrate control. Slc38a3 and Slc38a5 transfected cells release significantly more glutamine than mock-transfected cells. Co-incubation of the cells with ammonium significantly reduces glutamine efflux by both transporters. Note that MeAIB release is not increased by Slc38a3 or Slc38a5 transfected cells nor changed by pre-incubation in ammonium. In A-C all graphs show mean values with SEM. Significance were assessed by two-tailed *t*-tests and significant *P*-values are indicated by asterisks where $*P < .05$ and $***P < .001$

contain glial fibrillary acidic protein (GFAP) and glutamine synthetase, provide functional and structural support to retinal neurons and synaptic activity (eg, by neurotransmitter recycling and regulating ionic balance), and harbor endogenous Slc38a3 and Slc38a5 activities.[37-41] We therefore made primary cultured Müller glia cells and incubated them with the pH-sensitive dye BCECF and exposed them to glutamine followed by ratiometric analyses. The Müller glia cells show alkalinization (Figure 3A,B). This is consistent with a net pH change due to activation of the transport-coupled counter-transport of H^+ and uncoupled H^+ fluxes.[14-16] When Müller glia cells are pre-incubated with NH_4^+ followed by addition of glutamine, the glutamine-mediated alkalinization is extinguished (Figure 3B). This rules out the possibility that the alkalinization is merely an effect of NH_4^+-mediated pH changes and underpin that NH_4^+ inhibits the system N transporters in Müller glia cells.

In PS120 cells expressing one of the two system N transporters, ratiometric analyses also reveal glutamine-induced net alkalinization at resting membrane potential (Figure 3C,D), which is in harmony with previous reports.[15,16] Co-incubation with 0.5 mM NH_4^+ hampers glutamine-induced alkalinization (Figure 3C,D). With 1 mM NH_4^+ glutamine-induced alkalinization is abolished, suggesting that both coupled (ie, in symport with glutamine transport) and uncoupled H^+ fluxes through Slc38a3 and Slc38a5 are inhibited (Figure 3C,D). Altogether, our data show that even 0.5 mM NH_4^+ significantly reduce transport activities and competes with cations for the permeation pathways of the system N transporters in mammalian cells. As 0.5 mM NH_4^+ concentrations have been reported in the brains of HE patients[42-44] and of rats with experimentally induced ALF,[45,46] these results further bolster their clinical relevance.

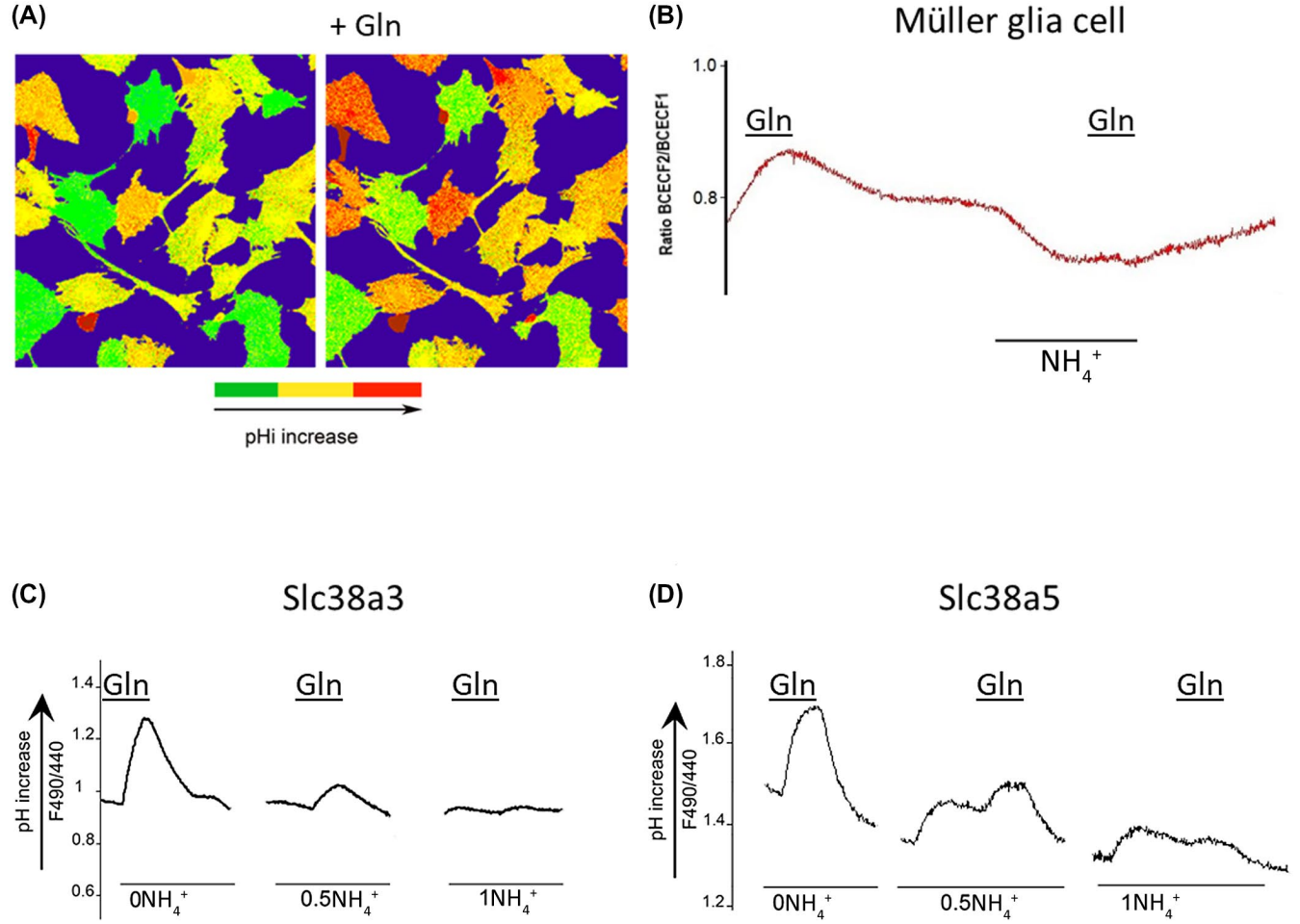

FIGURE 3 Ammonium abolishes Slc38a3- and Slc38a5-mediated cellular alkalinization. Cultured Müller glia cells or PS120 cells stably transfected for Slc38a3 or Slc38a5 were loaded with the H^+-sensitive dye BCECF and stimulated with glutamine in the absence or presence of ammonium prior to ratiometric analyses. A, Slc38a3 and Slc38a5 expressing rat Müller glia cells show increase in intracellular pH when stimulated with glutamine. B, pH trace from one representative Müller glia cell is shown. Glutamine induces alkalinization. Addition of NH_4^+ reduces pH_i. The glutamine-induced alkalization is obliterated upon addition of glutamine in the presence of NH_4^+. C-D, Slc38a3 and Slc38a5 expressing PS120 cells show glutamine-induced increase in intracellular pH which returns to baseline upon removal of glutamine. Upon co-application of glutamine with ammonium, the intracellular alkalinization is significantly reduced at 0.5 mM NH_4^+ and disappears at 1 mM NH_4^+ (effects of mere NH_4^+ are deducted). Representative traces are shown from one cell each

3.3 | NH_4^+ interacts with the Slc38 transporters and reduces the affinity of the system N transporters for glutamine

We hypothesized that NH_4^+ imposes its effect on the Slc38 transporters by direct interaction with the proteins. To this end, we applied the Drug Affinity Responsive Target Stability (DARTS) assay.[27] Incubation of cell lysates with the metalloproteinase thermolysin degrades all four Slc38 transporters as judged from protein immunoblots (Figure 4A). Pre-incubation of the lysates with NH_4^+ mitigates the reduction in staining for several of the transporters in accordance with physical interaction between NH_4^+ and the transporters, thereby reducing their susceptibility to thermolysin action—that is NH_4^+ stabilizes Slc38a2, Slc38a3, and Slc38a5 significantly while it fails to stabilize Slc38a1 (Figure 4B).

We next asked whether NH_4^+ regulates the transport by interfering with the substrate-binding sites. We therefore measured voltage-current dependence upon increasing glutamine concentrations with or without NH_4^+ in *X. laevis* oocytes expressing one of the four Slc38 transporters. NH_4^+ has no effect on the K_m for glutamine or V_{max} for the system A transporters (Table 1). By contrast, there is a highly significant increase in the K_m for glutamine for the system N transporters, while there is no change in V_{max} (Table 1). This implies that NH_4^+ competes with glutamine for the binding, selectively on the system N transporters.

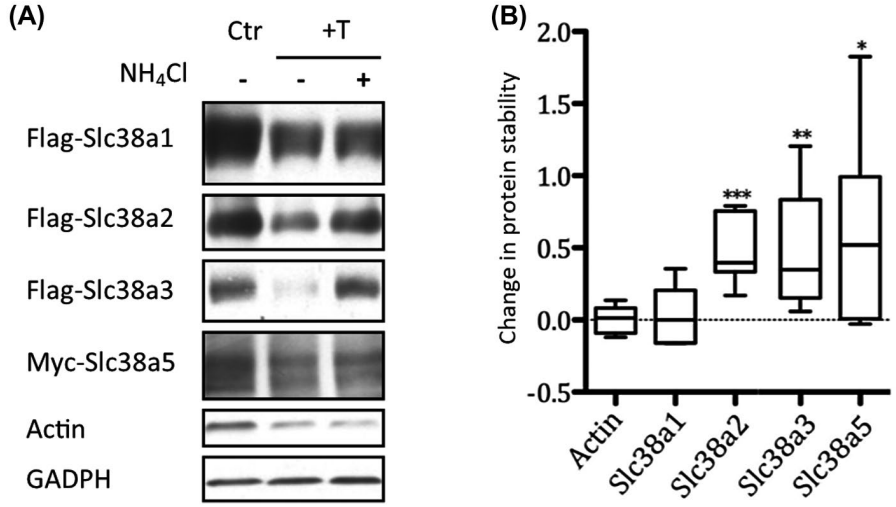

FIGURE 4 NH_4^+ physically interacts with Slc38 transporters. Human embryonic kidney (HEK) cells were transfected with either of four N-terminal tagged (Flag or Myc) Slc38 transporters and incubated for 48 hours. Drug Affinity Responsive Target Stability (DARTS) was applied to identify potential targeting of ammonium to the Slc38 transporters: Ammonium and/or glutamine were applied to the cells 5 minutes prior to mild lysis while keeping the cells on ice. The treatment conditions were maintained in the lysis buffer. Samples were then treated with 10 μg/mL thermolysin (T) for 10 minutes at room temperature and subsequently immunoblotted with antibodies for FLAG or MYC-tag. A, The Slc38 transporters investigated show degradation to some degree upon application of thermolysin. Addition of ammonium in the incubation buffer attenuates degradation of several of them. Actin and GAPDH are stained as positive and negative controls, respectively. B, DARTS data with thermolysin in A were quantified and expressed as relative change in staining intensity in NH_4^+ treated samples compared with samples without NH_4^+. Slc38a2, Slc38a3, and Slc38a5 are all significantly more stable with ammonium treatment. Boxplots indicate median values with the boxes spanning from the first to the third quartile. In B mean values with SEM are shown. The significance were assessed by one sample *t*-tests and significant *P*-values are indicated by asterisks where $*P < .05$, $**P < .01$, and $***P < .001$

TABLE 1 NH_4^+ significantly increases K_m of the system N transporters Slc38a3 and Slc38a5

		Km w/o NH^{4+}	Km w NH^{4+}	*P*	Vmax w/o NH^{4+}	Vmax with NH^{4+}	*P*
System A	Slc38a1	1.51 ± 0.002	1.77 ± 0.231	.223	0.217 ± 0.050	0.215 ± 0.045	.711
	Slc38a2	1.46 ± 0.164	1.77 ± 0.313	.210	0.195 ± 0.019	0.193 ± 0.005	.823
System N	Slc38a3	1.45 ± 0.122	3.29 ± 0.101	<.001	0.185 ± 0.010	0.172 ± 0.026	.352
	Slc38a5	1.53 ± 0.000	3.35 ± 0.226	.002	0.201 ± 0.067	0.196 ± 0.062	.328

Note: Xenopus laevis oocytes expressing one of four Slc38 glutamine transporters were stimulated with increasing glutamine concentrations before and after addition of ammonium. The generated currents were measured by two-electrode voltage-clamp electrophysiology. K_m and V_{max} were calculated for individual oocytes (n = 3). The table gives data obtained at −70 mV and the statistical power upon changes with ammonium treatment.

Abbreviation: w/o, without.

3.4 | NH_4^+ downregulates Slc38a3 transporters

We tested whether ammonium ions regulate membrane trafficking of the Slc38a3 transporter. HEK cells transiently transfected for Slc38a3 were incubated with 2 mM or 5 mM NH_4^+ for 0.5 or 2.0 hours followed by quantitative immunoblotting of the cell lysates. Compared with control cells, Slc38a3 protein content is reduced upon incubation with NH_4^+ (Figure 5A). HEK cells transfected for Slc38a3 were also fixated and stained for Slc38a3 by immunofluorescence. In the absence of NH_4^+, the staining for Slc38a3 is enriched at the cell membrane (Figure 5B). This staining is significantly reduced upon exposure of the cells to NH_4^+ for 0.5 hours. After 2 hours with ammonium ions, most of the cell membrane staining is vanished (Figure 5B). Thus, our data suggest that NH_4^+ downregulates Slc38a3 transporter in a time-dependent manner.

3.5 | Slc38a3 knockdown induces signs of cytotoxic edema and perturbs astroglia-to-neuron shuttling of glutamine

Our data have identified the astroglial system N transporters as a major target for NH_4^+ toxicity. To test whether

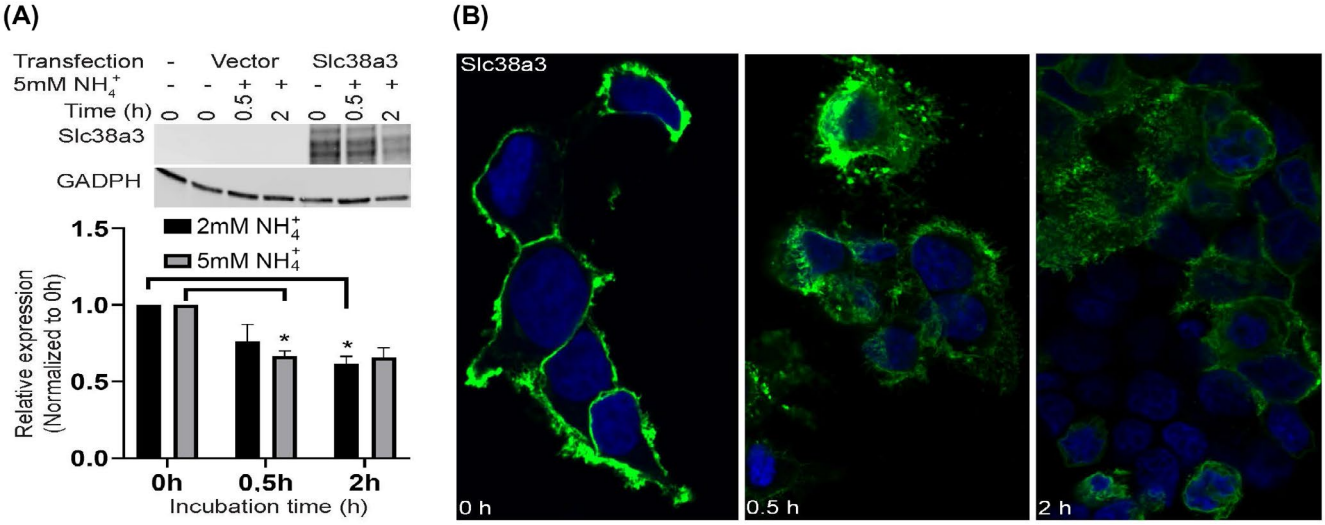

FIGURE 5 NH_4^+ downregulates Slc38a3 in Human Embryonic Kidney (HEK) cells. HEK cells transiently transfected for Slc38a3 were treated with 2 or 5 mM NH_4Cl for 0, 0.5, or 2 hours followed by cell lysis for quantitative immunoblotting or immersion fixation for immunofluorescence staining. A, Quantification of the immunoreactivity for Slc38a3 show that it is gradually reduced to reach significant levels in the presence of NH_4^+. The insets above the graphs show blots from a representative experiment stained for Slc38a3 and the house keeping gene glyceraldehyde 3-phosphate dehydrogenase (GADPH). B, In the absence of ammonium, laser scanning confocal microscopy shows strong staining for Slc38a3 at the cell membranes. Upon exposure of the cells to ammonium the cell membrane staining for Slc38a3 is significantly reduced after 0.5 hours and further decreased at 2 hours. A show mean values with SEM from three experiments. Two-way ANOVA was performed using the Dunnett's and Sidak's multiple comparison test. Significant *P*-values are indicated by asterisks where $*P < .05$. Green: staining for Slc38 isoforms; blue: DaPi

dysfunctional Slc38a3 in vivo may evoke pathophysiological symptoms of ALF, we infused Slc38a3-VM unilaterally in the frontal cortex of mice to silence Slc38a3 transporters. Quantitative western blotting shows ~50% reduction in Slc38a3 protein compared with the corresponding region in the contralateral hemisphere subjected to scrambled oligonucleotides (C-VM), suggesting a successful knockdown of Slc38a3 protein (Figure 6A).

Astroglial swelling and cytotoxic brain edema are hallmarks of ALF.[1] We therefore investigated peri-capillary astroglial processes by transmission electron microscopy (EM) at the sites of local Slc38a3 protein silencing and the corresponding regions in the contralateral hemisphere infused with C-VM. The size of peri-vascular astroglial cells and their appearance in the C-VM mice are comparable to earlier EM investigations of peri-capillary astroglial endfeet in wild-type rats (Figures. 6C and S1).[47,48] By contrast, peri-vascular astroglial processes in the Slc38a3-VM mice increase significantly in size and have a more electrolucent cytoplasm, indicating astroglial swelling (Figures 6D and S1).

Water diffusion was evaluated by magnetic resonance spectroscopy (MRS): Apparent Diffusion Coefficient (ADC) in Slc38a3-VM mice show a significant decrease (~ 18%; 0.743 ± 0.141 and 0.612 ± 0.082 $\mu m^2/s$ in control and Slc38a3-VM animals, respectively, $n = 6$) (Figure 6B).

We then assessed the impact of partial Slc38a3 knockdown by measuring the extracellular amino acid concentrations in the microdialysates (Figure 6E): Brain cortices from Slc38a3-VM reveal a significant decrease in glutamine (~40%) consistent with hampered Slc38a3 activity. A significantly increased level of the osmolyte taurine is seen in the microdialysates from Slc38a3-VM compared with C-VM, suggesting edema development (Figure 6E). Finally, metabolite concentrations in the cortices of Slc38a3-VM mice measured by MRS show a significant reduction in tissue glutamate (~12%) consistent with Slc38a3 being an important supplier of glutamine for the synthesis of glutamate (Figure 6F). Significant increase (~20%) in the phosphocholine concentration, a marker for edema, further corroborates edema development (Figure 6F). Thus, astrocytic swelling, ADC reduction, and increased brain phosphocholine and extracellular taurine and reduced extracellular glutamine and tissue glutamate in Slc38a3-VM underpin involvement of Slc38a3 in the development of cytotoxic edema and perturbed shuttling of glutamine from astroglia to neuron, suggesting a similar mechanistic development in ALF.

3.6 | Slc38a3 protein expression is significantly reduced in AOM-injected mice—a mouse model for human ALF

AOM-induced ALF in mice reproduces most of the neurological and biochemical features of human ALF (time-dependent

deterioration of neurological scores). Serum and CSF ammonia concentrations measured after sample collection and preparation indicated hyperammonemia (Table 2), in line with the documented increase in TNF-α and IL-1β levels in serum, increased activity of alanine and aspartate transaminases, elevated total glutamine and elevated extracellular glutamate levels.[28,49] We hypothesized that if system N transporters are involved in the pathogenesis of ALF, their activity should be affected in the AOM mice. First, we investigated the mice for ALF features. Water diffusion imaging by MRS showed a ~ 10% decrease in ADC in AOM-treated mice (Figure 7A; 0.676 ± 0.057 and 0.613 ± 0.081 $\mu m^2/s$ in control and in AOM-injected animals, respectively, mean ± SD n = 9). EM of frontal cortices from AOM mice shows enlarged and electron-lucent peri-vascular end-feet (Figure 7B, C; S2). The endothelium was also morphologically changed with numerous pinocytotic vesicles in the cytoplasm and microvilli on the luminal surface. Thus, the morphological changes and reduction in ADC are consistent with cytotoxic edema and with ALF.

Second, we examined system N transport activity. Fractional release of L-[^{3}H]glutamine in cortical slices

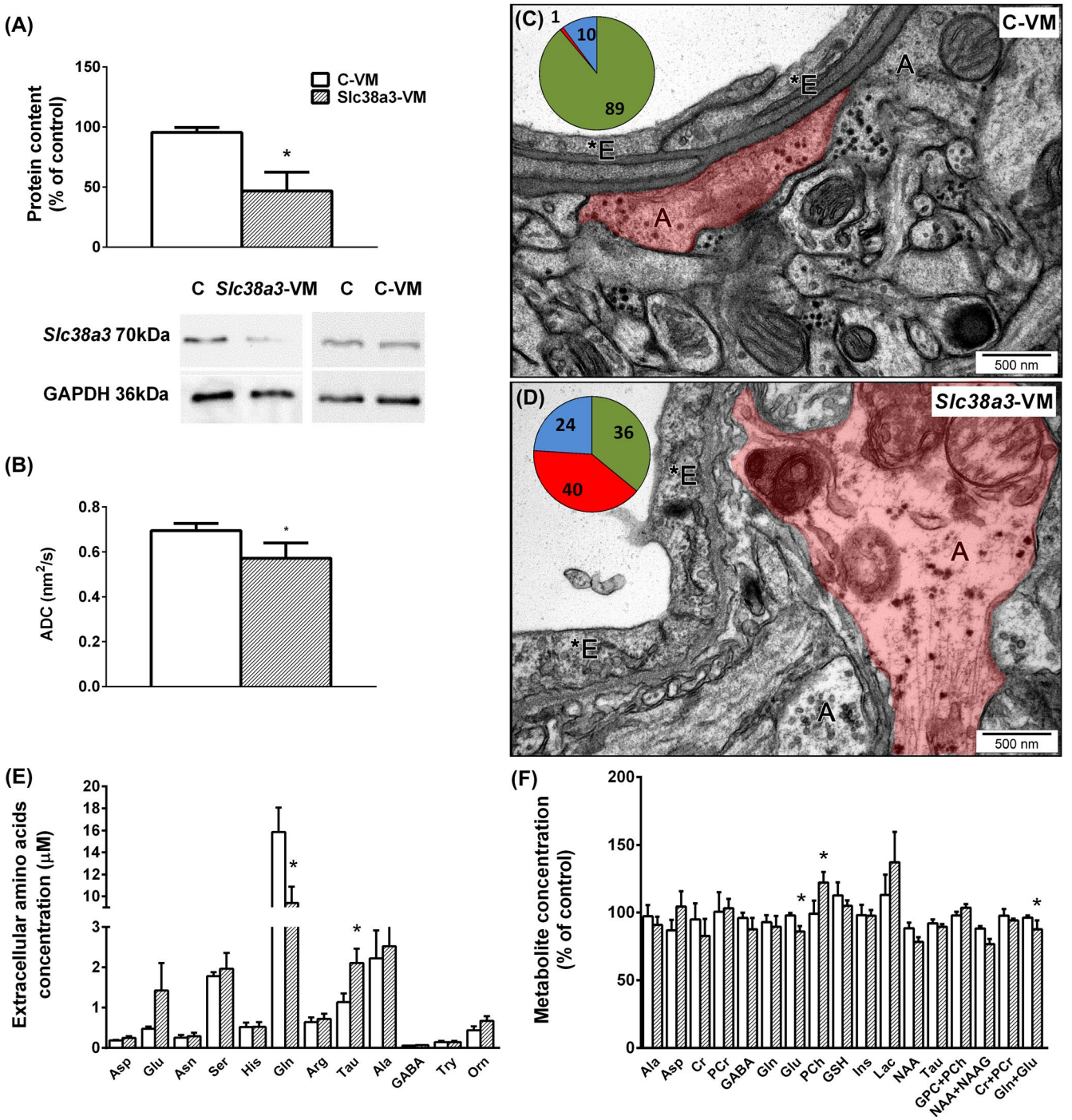

FIGURE 6 Slc38a3 silencing by vivo-morpholino (VM) leads to edema development, reduced extracellular glutamine levels, and reduced total brain glutamate. Osmotic mini-pumps were surgically implanted under the skin of mice which continuously infused anti-Slc38a3 VM oligonucleotides (Slc38a3-VM) or control mismatched-VM (C-VM) into the frontal cortex by means of a cannula for 4 days. A, Whole-brain extracts from mice undergone one of the treatments were made in SDS, separated in SDS–PAGE, stained for Slc38a3 followed by quantification of the immunoblots. Slc38a3 is significantly reduced in mice infused with Slc38a3-VM compared with C-VM. Representative immunoblots from Slc38a3-VM and C-VM mice stained for Slc38a3 or the housekeeping GAPDH protein are shown below the bar graph. $*P < .05$ vs. C-VM (*T*-test). n = 4. B, The diffusion of water molecules through the brains of Slc38a3-VM and C-VM mice was investigated by magnetic resonance spectroscopy. A significant reduction in the apparent diffusion coefficient (ADC) is measured in Slc38a3-VM compared with C-VM mice. $*P < .05$ vs. C-VM (*T*-Test). n = 15 C-D, C-VM and Slc38a3-VM mice were killed by perfusion fixation with 2% paraformaldehyde and 2.5% glutaraldehyde and their frontal cortices were dissected out and embedded in Epon 812. Electron microscopic investigation shows more electron lucidity and enlargement of the perivascular astroglial (A) end-feet in Slc38a3-VM mice compared with C-VM mice. The pie diagram summarizes the relative morphological findings of capillary vessels and structures around them in C-VM and Slc38a3-VM treated brains: Blood vessel profiles with unchanged ultrastructure (green), perivascular astrocytic projections with visible edema features (red), and blood vessels with changes on the endothelium, pinocytotic vesicles, unsealed connections between endothelial cells and thickened basal membranes (blue). E, Amino acid concentrations in microdialysates were measured in a pertinent region of Slc38a3-VM and C-VM mice by high-performance liquid chromatography. Glutamine is significantly reduced, while taurine is significantly increased. Note that glutamate shows a sub-significant increase. $*P < .05$ vs. C-VM (*T*-test) n = 5. F, Absolute metabolite concentration in the frontal cortex of Slc38a3-VM and C-VM mice was measured by proton magnetic resonance spectroscopy in pertinent brain regions compared with the metabolite level in the mirror part of the second hemisphere. Glutamate is significantly reduced, while phosphocholine is significantly increased in SN1-VM mice. $*P < .05$ vs. C-VM (*T*-test), n = 5

TABLE 2 Increased ammonia level in CSF and serum of AOM mice

	CSF (mmol)	Serum (mmol)
Control	0.20 ± 0.04	0.13 ± 0.02
AOM	0.34 ± 0.04*	0.55 ± 0.16*

Note: Right after samples collection and preparation ammonia level was measured spectrophotometrically. $*P < .05$ vs Control (*T*-test), n = 5 for CSF and n = 6 for serum.

obtained from AOM mouse brain was reduced in the eluates collected from fractions 1 to 5, compared with the release from control slices (Figure 7D). To identify the specific glutamine transport system disrupted in the AOM mice, we measured glutamine efflux in 4-minute pulses. Glutamine release is significantly reduced (~20%) in the AOM mice compared with control mice (Figure 7E). Incubation of the slices with excessive alanine and leucine to inhibit system A and system L activities, respectively, has no effect on the relative reduction in glutamine release (Figure 7E). Incubation of the slices with the competitive system N inhibitor L-glutamic acid-γ-monohydroxamate (GAH)[50,51] eliminates the difference between AOM and control mice, suggesting that system N is responsible for this difference in the AOM (Figure 7E).

Third, as proof of the concept that the activity of the system N transporters is downregulated in AOM mice, we measured expression of the Slc38a3 transporter. AOM significantly reduced its expression at both mRNA (~32%) and protein levels (~30%), respectively (Figure 7F). By contrast, the system A transporter Slc38a2 do not show downregulation in the AOM mice (Figure 7G), corroborating isoform-specific impact on system N transport in AOM mice.

4 | DISCUSSION

Our multidisciplinary study reveals involvement of Slc38 transporters in the pathogenesis of HE in three ways: First, we demonstrate that NH_4^+ interacts with and perturbs function of Slc38 transporters involved in the replenishment of the neurotransmitters glutamate and GABA: NH_4^+ impairs bidirectional astroglial glutamine transport by Slc38a3 and Slc38a5 and competes with cations (eg, K^+) for permeation through the same transporters. Second, knockdown of Slc38a3 in mice leads to development of astroglial swelling—a cardinal symptom of ALF—and reduced extracellular levels of glutamine and total brain glutamate concentration, consistent with perturbed astroglial-to-neuronal shuttling of glutamine. Third, AOM mice—a model for ALF—have reduced Slc38a3 protein expression, impeded glutamine release, and present astrocyte swelling. Thus, we have bolstered a role for Slc38 transporters in the pathogenesis of ALF: excessive accumulation of ammonia in brain of ALF mice hampers function and/or expression of Slc38 transporters, and impairment of Slc38 transporters leads to development of cardinal symptoms of ALF. The data are rigorous as they are underpinned by a multidisciplinary approach (TEVC, uptake- and efflux assays, ratiometric analyses, electron microscopy, magnetic spectroscopy, microdialyses and more), and the effects of ammonia on Slc38 transporters have been demonstrated in multiple in vitro cell systems, primary Müller glia cells, and in vivo mouse models for ALF to rule out any cell-specific peculiarities or artefacts and to show clinical relevance.

4.1 | Differential action of NH_4^+ on System A and System N transporters

We have demonstrated that NH_4^+ reduces the affinity of the Na^+/H^+-coupled System N transporters for glutamine (ie, K_m increases), while there is no effect on the V_{max}. By contrast, NH_4^+ has barely any effect on the kinetics of the Na^+-coupled System A transporters. We have previously shown that cations act on the Slc38 transporters in multiple ways: (1) The four Slc38 transporters have ordered binding of their substrates with Na^+ binding before the binding of the amino acid, (2) Li^+ can replace Na^+, (3) H^+ competes at the Na^+-binding sites, (4) coupled countertransport of H^+ makes the system N transporters electroneutral allowing them to work bidirectionally, and (5) the Slc38 transporters, in particular the system N transporters, permit uncoupled cation fluxes.[14,15,16,24,25] We now show that unlike the smaller cation H^+, NH_4^+ interacts with the amino acid-binding sites selectively at the Na^+/H^+-coupled System N transporters in a competitive manner. In addition, NH_4^+ also permeates through the system N transporters. The latter harmonizes well with the demonstrated channel-like activities associated

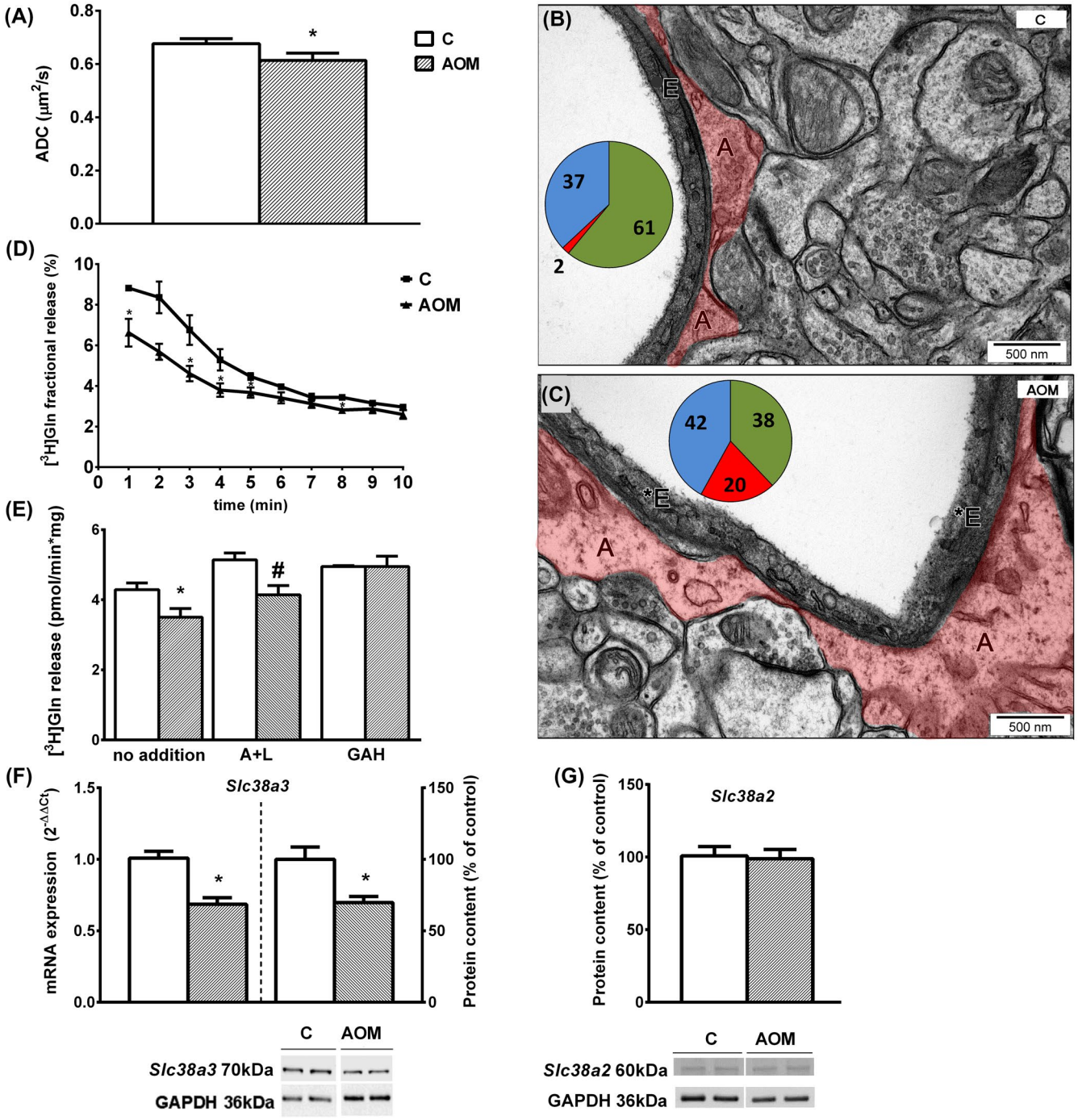

FIGURE 7 Azoxymethane (AOM)-induced acute liver failure in mice shows cytotoxic edema and downregulation of Slc38a3 activity. A, Diffusion of water molecules through the brains of AOM-treated or untreated mice was measured by magnetic resonance spectroscopy. There is a significant (~10%) reduction in the apparent diffusion coefficient (ADC) in AOM mice compared with the control (C) mice. *$P < .05$ vs. C (*T*-test); n = 9. B-C, AOM treated mice (AOM; n = 4) and untreated control mice (C; n = 4) were perfusion fixed and small pieces of brain tissue from the frontal cortices were dissected out and embedded in Epon 812. Ultrathin sections were cut by an ultramicrotome and investigated by transmission electron microscopy (EM). Enlarged and electron-lucent astroglial (A) end-feet around blood vessels (red pseudocolor), numerous pinocytic vesicles in the endothelial cells (E) and disrupted endothelial layer (*) are detected in the frontal cortices of the AOM mice. The relative morphological findings of capillary vessels and structures around them in C- and AOM brains are summarized in the pie diagram: Blood vessel profiles and surroundings with unchanged ultrastructure (green), astrocytic projections with visible features of edema (red) and morphologically changed endothelium with numerous pinocytotic vesicles in cytoplasm and microvilli on the luminal surface of endothelial cells (blue). D, Fractional release of glutamine from slices was measured in 1-min perfusate samples and expressed as the percentage of glutamine released in relation to the total initial content of the slice loaded with [^{3}H]glutamine. *$P < .05$ vs. control mice (C) at the same time point, (*T*-test) n = 6. E, Mean glutamine efflux was measured during a 4-min pulse in the presence of alanine and leucine (A + L), L-glutamic acid-γ-monohydroxamate (GAH) or without any supplement, per 1 minutes. A relative reduction in glutamine efflux is seen in AOM mice compared to controls when no agonists or antagonists are added or when excess alanine and leucine are added. The addition of GAH obliterates glutamine release in wild type mice. *indicates $P < .05$ vs. control with no addition, #$P < .05$ vs. control after A+ L pulse, (*T*-test) n = 5. F, Quantitative analysis of Slc38a3 shows a significant reduction of its expression at both the mRNA and protein level in the AOM mice compared with C mice. G, Quantification of Slc38a2 protein levels in C and AOM mice did not reveal any significant change. Representative electrophorograms of Slc38a2, Slc38a3 and housekeeping protein GAPDH are shown at the bottom of F and/or G. *$P < .05$ vs. C mice, (*T*-test) n = 8

with system N transporters allowing uncoupled fluxes of cations such as K^+, Na^+, and H^+.[15,16,33,35] Indeed, NH_4^+ and K^+ are similar in size and charge,[52] and it is plausible that they are translocated through the same channels. NH_4^+ may therefore compete with uncoupled K^+ fluxes through system N transporters contributing to impaired astroglial K^+ buffering.

4.2 | Impaired function of Slc38 glutamine transporters is required for the pathogenesis of ALF

To unravel the pathogenesis of HE, we induced fulminant hepatic failure by injecting AOM intraperitoneally in mice.[49] This acutely interrupts both urea and glutamine-mediated detoxification of NH_4^+ in the liver and is followed by accumulation of NH_4^+ in the serum and a high load to the brain congruous with ALF.[28,49] The brains of these mice displayed reduced expression of Slc38a3 together with impaired system N-dependent astroglial glutamine release. These data are corroborated by Slc38a3 knockdown in mice showing reduced glutamine in the microdialysate and reduced total glutamate concentrations in the brain. Thus, our findings imply an inhibition of the astroglial system N transporters Slc38a3 and Slc38a5 and disruption of glutamine transport from astroglia to neurons in the pathogenesis of ALF, as less system N-mediated astroglial glutamine release reduces the extracellular levels of glutamine. Consequently, there is reduced glutamine transport into neurons for the formation of glutamate. The sustained total brain glutamine despite reduced microdialysate glutamine, and reduced astrocytic glutamine release suggests that glutamine is accumulated inside astroglial cells. This glutamine may then exert osmotic effects according to the osmotic gliopathy theory[11] and/or be transported into the mitochondria with potential formation of NH_4^+, production of reactive oxygen and nitrosative species, mitochondrial dysfunction and astrocyte swelling according to the Trojan Horse theory.[12] In addition, NH_4^+ penetrating through Slc38a3 and Slc38a5 may change intracellular pH and membrane potential and thereby regulate a wide range of intracellular proteins, leading to further astroglial dysfunction.

Thrane and co-workers have demonstrated that NH_4^+ impairs astrocyte K^+-buffering by competing for Na^+/K^+-ATPase uptake so that extracellular K^+ concentration increases.[13] Subsequently, this increased K^+ level overactivates the neuronal Na^+-K^+-$2Cl^-$ co-transporter isoform 1 (NKCC1) resulting in depolarization of the GABAergic reversal potential in cortical pyramidal cells, impairing inhibitory networks. We show that NH_4^+ competes with K^+ for penetration through the system N transporters and may thus contribute to reduced astrocytic K^+-buffering. This may also have an impact on GABAergic reversal potential and thereby on inhibitory networks. Our data are thus consistent with altered and fluctuating glutamatergic and GABAergic neurotransmission reported for HE.[13,53,54]

Interestingly, disruption of the activity of Slc38 transporters and the ensuing glutamine shuttle by NH_4^+ are acute and occur within the first hours. Furthermore, the associated enlarged peri-vascular astroglial processes and reduced ADC in mice in which Slc38a3 activity is knocked-down, as well as in a mouse model for ALF, are consistent with hyperammonemia-associated astroglial swelling,[10] which may transform astroglial membrane functions.[55,56] Indeed, hyperammonemia associated with ALF leads to cerebral edema and causes death more than in CLF.[1] Thus, impaired activity of Slc38 transporters and ensuing distortion of the astroglia-to-neuron glutamine shuttle may

be paramount for instigation of ALF pathogenesis. In addition, as the system N transporters are also expressed at the blood–brain barrier (BBB),[14,40,48,57,58,60] the glutamine equilibrium may also be distorted at the BBB further augmenting development of ALF.

5 | CONCLUDING COMMENTS

While the present study strongly suggests that distortion of Slc38 transporter function by NH_4^+ may be essential for development of ALF, the overall significance of the findings must be interpreted with caution. Slc38 transporters are differentially distributed in the brain,[17,19,20,40] so their contribution to the region-specific manifestations of the disease may vary. A recent study contributed by one of our laboratories demonstrated that SN1 silencing by a procedure used in the present study only partly impairs basic parameters of glutamatergic neurotransmission in the mouse frontal cortex.[59] It is likely that the involvement of transporter dysfunction will also be differentially accentuated in the different phases of the disease. This caveat may hold for both the neurotransmission status and astrocytic function. The above aspects need further investigation. On top of that, in future experiments, the role of transporter dysfunction will have to be evaluated against the complexity of various aspects of pathogenetic mechanism of HE, such as (1) differential regional regulation of ammonia-metabolizing enzymes,[60] (2) involvement of systemic inflammation, (3) immune dysfunction, (4) disruption of the BBB, (5) dysfunction of NKCC co-transporters,[1,13] to mention a few.

ACKNOWLEDGMENT

The authors thank Dr. Marivi N. Moen for contribution to immunofluorescene and western blotting data and Professor Emeritus Jon Storm-Mathisen for critical reading of the manuscript. We also thank Mrs Inez Fręśko for excellent contribution to transport analysis and Jarosław Orzeł, a former employee of the Small Animal Magnetic Resonance Imaging Laboratory Mossakowski Medical Research Centre PAS Warsaw, Poland for advice on MRI analysis. This work was funded by the National Centre for Research (NCBiR) Polish-Norwegian Research Program (No Pol-Nor/196190/23/2013), South-Eastern Norway Regional Health Authority (ID: 21561/2017052) and Molecular Life Science.

CONFLICT OF INTERESTS

The authors have no financial and/or non-financial interests in relation to the work described.

AUTHOR CONTRIBUTIONS

F.A. Chaudhry, M. Zielińska, J. Albrecht, E.H. Hamdani, and T.P. Utheim designed research. E.H. Hamdani, M. Popek, and M. Frontczak-Baniewicz performed research. T.P. Utheim contributed new reagents or analytic tools. All authors analyzed data: F.A. Chaudhry, M. Zielińska, and J. Albrecht wrote the paper.

ORCID

Mariusz Popek https://orcid.org/0000-0003-4394-3394
Małgorzata Frontczak-Baniewicz https://orcid.org/0000-0001-5676-3347
Jan Albrecht https://orcid.org/0000-0001-6063-6228
Magdalena Zielińska https://orcid.org/0000-0001-7388-3092
Farrukh Abbas Chaudhry https://orcid.org/0000-0002-2039-9667

REFERENCES

1. Aldridge DR, Tranah EJ, Shawcross DL. Pathogenesis of hepatic encephalopathy: role of ammonia and systemic inflammation. *J Clin Exp Hepatol*. 2015;5:S7-S20.
2. Felipo V. Hepatic encephalopathy: effects of liver failure on brain function. *Nat Rev Neurosci*. 2013;14:851.
3. Felipo V, Butterworth RF. Neurobiology of ammonia. *Prog Neurogibol*. 2002;67:259-279.
4. Albrecht J, Jones EA. Hepatic encephalopathy: molecular mechanisms underlying the clinical syndrome. *J. Neurol. Sci*. 1999;170:138-146.
5. Swain M, Butterworth RF, Blei AT. Ammonia and related amino acids in the pathogenesis of brain edema in acute ischemic liver failure in rats. *Hepatology*. 1992;15:449-453.
6. Scott TR, Kronsten VT, Hughes RD, Shawcross DL. Pathophysiology of cerebral oedema in acute liver failure. *World J Gastroenterol*. 2013;19:9240-9255.
7. Hakvoort TB, He Y, Kulik W, et al. Pivotal role of glutamine synthetase in ammonia detoxification. *Hepatology*. 2017;65:281-293.
8. Cooper AJ, Jeitner TM. Central role of glutamate metabolism in the maintenance of nitrogen homeostasis in normal and hyperammonemic brain. *Biomolecules*. 2016;6:1-33.
9. Martinez-Hernandez A, Bell KP, Norenberg MD. Glutamine synthetase: glial localization in brain. *Science*. 1977;195:1356-1358.
10. Willard-Mack CL, Koehler RC, Hirata T, et al. Inhibition of glutamine synthetase reduces ammonia-induced astrocyte swelling in rat. *Neuroscience*. 1996;71:589-599.
11. Brusilow SW, Koehler RC, Traystman RJ, Cooper AJ. Astrocyte glutamine synthetase: importance in hyperammonemic syndromes and potential target for therapy. *Neurotherapeutics*. 2010;7:452-470.
12. Albrecht J, Norenberg MD. Glutamine: a Trojan horse in ammonia neurotoxicity. *Hepatology*. 2006;44:788-794.
13. Rangroo TV, Thrane AS, Wang F, et al. Ammonia triggers neuronal disinhibition and seizures by impairing astrocyte potassium buffering. *Nat Med*. 2013;19:1643-1648.
14. Chaudhry FA, Reimer RJ, Krizaj D, et al. Molecular analysis of System N suggests novel physiological roles in nitrogen metabolism and synaptic transmission. *Cell*. 1999;99:769-780.
15. Chaudhry FA, Krizaj D, Larsen P, et al. Coupled and uncoupled proton movement regulates amino acid transport by System N. *EMBO J*. 2001;20:7041-7051.

16. Hamdani EH, Gudbrandsen M, Bjørkmo M, Chaudhry FA. The system N transporter SN2 doubles as a transmitter precursor furnisher and a potential regulator of NMDA receptors. *Glia*. 2012;60:167-1683.
17. Solbu TT, Bjorkmo M, Berghuis P, Harkany T, Chaudhry FA. SAT1, A Glutamine transporter, is preferentially expressed in GABAergic neurons. *Front Neuroanat*. 2010;4:1.
18. Qureshi T, Sørensen C, Berghuis P, et al. The glutamine transporter Slc38a1 regulates GABAergic neurotransmission and synaptic plasticity. *Cereb Cortex*. 2019;29:5166-5179..
19. Cubelos B, Gonzalez-Gonzalez IM, Gimenez C, Zafra F. Amino acid transporter SNAT5 localizes to glial cells in the rat brain. *Glia*. 2005;49:230-244.
20. Jenstad M, Quazi AZ, Zilberter M, et al. System A transporter SAT2 mediates replenishment of dendritic glutamate pools controlling retrograde signaling by glutamate. *Cereb. Cortex*. 2009;19:1092-1106.
21. Menchini RJ, Chaudhry FA. Multifaceted regulation of the system A transporter Slc38a2 suggests nanoscale regulation of amino acid metabolism and cellular signaling. *Neuropharmacology*. 2019;161:107789.
22. Malaguarnera M, Llansola M, Balzano T, et al. Bicuculline reduces neuroinflammation in hippocampus and improves spatial learning and anxiety in hyperammonemic rats. Role of glutamate receptors. *Front Pharmacol*. 2019;10:132.
23. Cittolin-Santos GF, Guazzelli PA, Nonose Y, et al. Behavioral, neurochemical and brain oscillation abnormalities in an experimental model of acute liver failure. *Neuroscience*. 2019;401:117-129.
24. Reimer RJ, Chaudhry FA, Gray AT, Edwards RH. Amino acid transport System A resembles System N in sequence but differs in mechanism. *Proc Natl Acad Sci USA*. 2000;97:7715-7720.
25. Chaudhry FA, Schmitz D, Reimer RJ, et al. Glutamine uptake by neurons: interaction of protons with system a transporters. *J Neurosci*. 2002;22:62-72.
26. Nissen-Meyer LSH, Popescu MC, Hamdani EH, Chaudhry FA. Protein kinase C-mediated phosphorylation of a single serine residue on the rat glial glutamine transporter SN1 governs its membrane trafficking. *J Neurosci*. 2011;31:6565-6575.
27. Lomenick B, Hao R, Jonai N, et al. Target identification using drug affinity responsive target stability (DARTS). *Proc Natl Acad Sci U.S.A*. 2009;106:21984-21989.
28. Popek M, Bobula B, Sowa J, et al. Cortical synaptic transmission and plasticity in acute liver failure are decreased by presynaptic events. *Mol Neurobiol*. 2018;55:1244-1258.
29. Zielinska M, Dabrowska K, Hadera MG, Sonnewald U, Albrecht J. System N transporters are critical for glutamine release and modulate metabolic fluxes of glucose and acetate in cultured cortical astrocytes: changes induced by ammonia. *J Neurochem*. 2016;136:329-338.
30. Livak KJ, Schmittgen TD. Analysis of relative gene expression data using real-time quantitative PCR and the 2(-Delta Delta C(T)) Method. *Methods*. 2001;25:402-408.
31. Provencher SW. Automatic quantitation of localized in vivo 1H spectra with LCModel. *NMR Biomed*. 2001;14:260-264.
32. Hilgier W, Zielinska M, Borkowska HD, et al. Changes in the extracellular profiles of neuroactive amino acids in the rat striatum at the asymptomatic stage of hepatic failure. *J Neurosci Res*. 1999;56:76-84.
33. Schneider HP, Broer S, Broer A, Deitmer JW. Heterologous expression of the glutamine transporter SNAT3 in Xenopus oocytes is associated with four modes of uncoupled transport. *J Biol Chem*. 2007;282:3788-3798.
34. Marcaggi P, Coles JA. Ammonium in nervous tissue: transport across cell membranes, fluxes from neurons to glial cells, and role in signalling. *Prog Neurogibol*. 2001;64:157-183.
35. Broer A, Albers A, Setiawan I, et al. Regulation of the glutamine transporter SN1 by extracellular pH and intracellular sodium ions. *J Physiol*. 2002;539:3-14.
36. Burckhardt BC, Burckhardt G. NH4+ conductance in Xenopus laevis oocytes. I. Basic observations. *Pflugers Arch*. 1997;434:306-312.
37. Chang ML, Wu CH, Jiang-Shieh YF, Shieh JY, Wen CY. Reactive changes of retinal astrocytes and Muller glial cells in kainate-induced neuroexcitotoxicity. *J Anat*. 2007;210:54-65.
38. Goldman D. Muller glial cell reprogramming and retina regeneration. *Nat Rev Neurosci*. 2014;15:431-442.
39. Reichenbach A, Bringmann A. New functions of Muller cells. *Glia*. 2013;61:651-678.
40. Boulland JL, Osen KK, Levy LM, et al. Cell-specific expression of the glutamine transporter SN1 suggests differences in dependence on the glutamine cycle. *Eur J Neurosci*. 2002;15:1615-1631.
41. Umapathy NS, Dun Y, Martin PM, et al. Expression and function of system N glutamine transporters (SN1/SN2 or SNAT3/SNAT5) in retinal ganglion cells. *Invest Ophthalmol Vis Sci*. 2008;49:5151-5160.
42. Butterworth RF, Giguere JF, Michaud J, Lavoie J, Layrargues GP. Ammonia: key factor in the pathogenesis of hepatic encephalopathy. *Neurochem Pathol*. 1987;6:1-12.
43. Bhatia V, Singh R, Acharya SK. Predictive value of arterial ammonia for complications and outcome in acute liver failure. *Gut*. 2006;55:98-104.
44. Niranjan-Azadi AM, Araz F, Patel YA, et al. Ammonia level and mortality in acute liver failure: a single-center experience. *Ann Transplant*. 2016;21:479-483.
45. Hilgier W, Olson JE. Brain ion and amino acid contents during edema development in hepatic encephalopathy. *J Neurochem*. 1994;62:197-204.
46. Mans AM, DeJoseph MR, Hawkins RA. Metabolic abnormalities and grade of encephalopathy in acute hepatic failure. *J Neurochem*. 1994;63:1829-1838.
47. Chaudhry FA, Lehre KP, Van Lookeren Campagne M, Ottersen OP, Danbolt NC, Storm-Mathisen J. Glutamate transporters in glial plasma membranes: highly differentiated localizations revealed by quantitative ultrastructural immunocytochemistry. *Neuron*. 1995;14:711-720.
48. Boulland JL, Rafiki A, Levy LM, Storm-Mathisen J, Chaudhry FA. Highly differential expression of SN1, a bidirectional glutamine transporter, in astroglia and endothelium in the developing rat brain. *Glia*. 2003;41:260-275.
49. Matkowskyj KA, Marrero JA, Carroll RE, Danilkovich AV, Green RM, Benya RV. Azoxymethane-induced fulminant hepatic failure in C57BL/6J mice: characterization of a new animal model. *Am J Physiol*. 1999;277:G455-G462.
50. Baird FE, Beattie KJ, Hyde AR, Ganapathy V, Rennie MJ, Taylor PM. Bidirectional substrate fluxes through the system N (SNAT5) glutamine transporter may determine net glutamine flux in rat liver. *J Physiol*. 2004;559:367-381.
51. Dolgodilina E, Imobersteg S, Laczko E, Welt T, Verrey F, Makrides V. Brain interstitial fluid glutamine homeostasis is controlled by blood-brain barrier SLC7A5/LAT1 amino acid transporter. *J Cereb Blood Flow Metab*. 2016;36:1929-1941.

52. Marcaggi P, Jeanne M, Coles JA. Neuron-glial trafficking of NH4+ and K+: separate routes of uptake into glial cells of bee retina. *Eur J Neurosci*. 2004;19:966-976.
53. Leke R, Bak LK, Iversen P, et al. Synthesis of neurotransmitter GABA via the neuronal tricarboxylic acid cycle is elevated in rats with liver cirrhosis consistent with a high GABAergic tone in chronic hepatic encephalopathy. *J Neurochem*. 2011;117:824-832.
54. Fleischer W, Theiss S, Schnitzler A, Sergeeva O. Glutamine triggers long-lasting increase in striatal network activity in vitro. *Exp Neurol*. 2017;290:41-52.
55. Kimelberg HK, Kettenmann H. Swelling-induced changes in electrophysiological properties of cultured astrocytes and oligodendrocytes. I. Effects on membrane potentials, input impedance and cell-cell coupling. *Brain Res*. 1990;529:255-261.
56. Kimelberg HK, Anderson E, Kettenmann H. Swelling-induced changes in electrophysiological properties of cultured astrocytes and oligodendrocytes. II. Whole-cell currents. *Brain Res*. 1990;529:262-268.
57. Ennis SR, Kawai N, Ren XD, Abdelkarim GE, Keep RF. Glutamine uptake at the blood-brain barrier is mediated by N-system transport. *J Neurochem*. 1998;71:2565-2573.
58. Lee WJ, Hawkins RA, Vina JR, Peterson DR. Glutamine transport by the blood-brain barrier: a possible mechanism for nitrogen removal. *Am J Physiol*. 1998;274:C1101-C1107.
59. Popek M, Bobula B, Sowa J, et al. Physiology and morphological correlates of excitatory transmission are preserved in glutamine transporter SN1-depleted mouse frontal cortex. *Neuroscience*. 2020;446:124-136.
60. Kosenko EA, Tikhonova LA, Reddy VP, Aliev G, Kaminsky YG. Differential up-regulation of ammonia detoxifying enzymes in cerebral cortex, cerebellum, hippocampus, striatum and liver in hyperammonemia. *CNS Neurol Disord Drug Targets*. 2014;13:1089-1095.

SUPPORTING INFORMATION

Additional Supporting Information may be found online in the Supporting Information section.

How to cite this article: Hamdani EH, Popek M, Frontczak-Baniewicz M, et al. Perturbation of astroglial Slc38 glutamine transporters by NH_4^+ contributes to neurophysiologic manifestations in acute liver failure. *The FASEB Journal*. 2021;35:e21588. https://doi.org/10.1096/fj.202001712RR